

Brain networks predict metabolism, diagnosis and prognosis at the bedside in disorders of consciousness

Srivas Chennu,^{1,2} Jitka Annen,³ Sarah Wannez,³ Aurore Thibaut,^{3,4} Camille Chatelle,^{3,5,6} Helena Cassol,³ Géraldine Martens,³ Caroline Schnakers,^{7,8} Olivia Gosseries,³ David Menon⁹ and Steven Laureys³

Recent advances in functional neuroimaging have demonstrated novel potential for informing diagnosis and prognosis in the unresponsive wakeful syndrome and minimally conscious states. However, these technologies come with considerable expense and difficulty, limiting the possibility of wider clinical application in patients. Here, we show that high density electroencephalography, collected from 104 patients measured at rest, can provide valuable information about brain connectivity that correlates with behaviour and functional neuroimaging. Using graph theory, we visualize and quantify spectral connectivity estimated from electroencephalography as a dense brain network. Our findings demonstrate that key quantitative metrics of these networks correlate with the continuum of behavioural recovery in patients, ranging from those diagnosed as unresponsive, through those who have emerged from minimally conscious, to the fully conscious locked-in syndrome. In particular, a network metric indexing the presence of densely interconnected central hubs of connectivity discriminated behavioural consciousness with accuracy comparable to that achieved by expert assessment with positron emission tomography. We also show that this metric correlates strongly with brain metabolism. Further, with classification analysis, we predict the behavioural diagnosis, brain metabolism and 1-year clinical outcome of individual patients. Finally, we demonstrate that assessments of brain networks show robust connectivity in patients diagnosed as unresponsive by clinical consensus, but later re-diagnosed as minimally conscious with the Coma Recovery Scale-Revised. Classification analysis of their brain network identified each of these misdiagnosed patients as minimally conscious, corroborating their behavioural diagnoses. If deployed at the bedside in the clinical context, such network measurements could complement systematic behavioural assessment and help reduce the high misdiagnosis rate reported in these patients. These metrics could also identify patients in whom further assessment is warranted using neuroimaging or conventional clinical evaluation. Finally, by providing objective characterization of states of consciousness, repeated assessments of network metrics could help track individual patients longitudinally, and also assess their neural responses to therapeutic and pharmacological interventions.

1 School of Computing, University of Kent, UK

2 Department of Clinical Neurosciences, University of Cambridge, UK

3 Coma Science Group, GIGA Consciousness, University and University Hospital of Liège, Liège, Belgium

4 Spaulding-Labuschagne Neuromodulation Center, Spaulding Rehabilitation Hospital, Department of Physical Medicine and Rehabilitation, Harvard Medical School, Boston, MA, USA

5 Department of Physical Medicine and Rehabilitation, Spaulding Rehabilitation Hospital and Harvard Medical School, Boston, MA, USA

6 Laboratory for NeuroImaging of Coma and Consciousness, Massachusetts General Hospital, Boston, MA, USA

7 Neurosurgery Department, University of California, Los Angeles, CA, USA

8 Research Institute, Casa Colina Hospital and Centers of Healthcare, Pomona, CA, USA

9 Division of Anaesthetics, University of Cambridge, UK

Correspondence to: Dr Srivas Chennu,
University of Kent, Chatham Maritime ME4 4AG,
UK
E-mail: sc785@kent.ac.uk

Keywords: disorders of consciousness; electroencephalography; positron emission tomography; resting state; brain networks

Abbreviations: AUC = area under the curve; CRS-R = Coma Recovery Scale-Revised; dwPLI = debiased weighted phase lag index; GOS-E = Glasgow Outcome Scale-Extended; MCS = minimally conscious state; SVM = support vector machine; UWS = unresponsive wakefulness syndrome

Introduction

Recent years have seen rapid advancement of research that has built the evidence base for neurotechnology in assessment of consciousness after brain injury, which can result in prolonged disorders of consciousness, including unresponsive wakefulness syndrome (UWS), minimally conscious state minus (MCS–) and positive minimally conscious state (MCS+). The exclusive use of clinical consensus of behaviours observed at the bedside has repeatedly been shown to result in high rates of misdiagnosis of the true level of consciousness in such patients (Childs *et al.*, 1993; Schnakers *et al.*, 2009). This misdiagnosis can be due to the inability to communicate with patients, who might have no or inconsistent behavioural signs of consciousness. To help address the diagnostic and prognostic challenge in disorders of consciousness, a range of neuroimaging technologies have been proposed for assessing ongoing brain activity with sophisticated analytical techniques. These include MRI (Demertzi *et al.*, 2015), PET (Thibaut *et al.*, 2012; Stender *et al.*, 2014) and high density EEG (Lehembre *et al.*, 2012; King *et al.*, 2013; Lechinger *et al.*, 2013; Chennu *et al.*, 2014; Sitt *et al.*, 2014).

EEG in particular is an attractive option in this context as it is portable, cost-effective, and relatively feasible to deploy at the patient's bedside. Recent research has shown that both qualitative assessment by experts (Forgacs *et al.*, 2014; Bagnato *et al.*, 2016; Estraneo *et al.*, 2016; Piarulli *et al.*, 2016) and quantitative assessment using quasi-automated machine learning (Sitt *et al.*, 2014) can be effective for identifying the state of consciousness based on ongoing electrical brain activity measured non-invasively from the scalp. Further work has also shown that the methodology for quantitative analysis of EEG data could be eventually entirely automated, enabling the estimation of the state of consciousness at the patient's bedside using a validated analytical pipeline (Engemann *et al.*, 2015). In this context, we have previously shown that quantitative analysis of high density EEG using network analysis tools developed for brain connectomics research (Rubinov and Sporns, 2010) can identify specific spectral signatures of reorganized brain networks in patients with disorders of consciousness (Chennu *et al.*, 2014).

To build on this work and advance the case for developing reliable clinically useful applications of such neurotechnology-based assessments in disorders of consciousness, key challenges have yet to be addressed. One particular question pertains to the extent to which assessments with different neuroimaging modalities are concordant with each other. This is particularly important as both false positives and false negatives can have serious clinical and ethical implications in each individual case (Peterson *et al.*, 2015). However, in the absence of a gold standard to identify the true subjective state of consciousness of a patient who does not exhibit reliable behavioural evidence of consciousness, an approach based on consilience between multiple independent assessments might be a rational way forward (Peterson, 2016).

Another question pertinent to understanding the real-world utility of bedside assessments of EEG is the extent to which it can complement clinical interpretation and management, by providing clinicians with additional, fine-grained information for more informed decision-making on behalf of individual patients. While previous research has demonstrated that EEG-based assessment of consciousness has diagnostic value, systematic behavioural assessment conducted by an expert using the Coma Recovery Scale-Revised (CRS-R) (Kalmar and Giacino, 2005) has often been used as the ground truth against which EEG-based assessments are evaluated for their efficacy. However, it has yet to be demonstrated that quantitative EEG assessments, if eventually deployed at the bedside, could in fact be used to complement the CRS-R at non-specialist centres that commonly assess patients with standard clinical examination.

A further issue worth considering is whether EEG assessments have prognostic value for predicting longer term recovery in patients. This has been shown with PET (Stender *et al.*, 2014) and hinted in previous research with EEG (Sitt *et al.*, 2014). If verified, it would speak to the value of repeatable EEG assessments in not only tracking the recovery of behaviourally evidenced awareness, but also their ability to detect progressive improvements in the underlying neurological functions that support such recovery before they can be observed at the bedside.

Here, we directly tackle these challenges aimed at elaborating the clinical utility of high density EEG assessments in disorders of consciousness. Combining a rich set of clinical,

behavioural, PET, and EEG data from a large cohort of patients, we test multiple hypotheses. These include the evaluation of EEG-based assessments for diagnosis and prognosis of consciousness in disorders of consciousness, the presence of concordance across EEG and PET (used here as a neuroimaging reference method), and the role for EEG to complement systematic behavioural assessment at the bedside. Further, we train and validate classification algorithms that use EEG-derived metrics as inputs to predict the behavioural diagnosis, brain metabolism and clinical outcomes of individual patients with high accuracy.

Materials and methods

Participants

We assessed the level of consciousness, prognosis and treatment options of patients referred to the University Hospital of Liège, Belgium. Patients were referred from clinical centres across Europe. Data from patients referred between January 2008 and October 2015, either diagnosed with a disorder of consciousness, or having emerged from one, were included.

The study was approved by the Ethics Committee of the University Hospital of Liège. Patients' legal guardians gave written informed consent. Patients with locked-in syndrome were included as a clinically relevant group for comparison (Supplementary material). We also collected data from healthy controls as a reference group, all of whom gave informed written consent before participation. There were no significant differences between patients and controls in gender or age.

Neurobehavioural and PET assessments

Patients were assessed on the day of the PET and EEG assessments using the CRS-R. A patient's diagnosis was based on the highest score obtained over five to seven CRS-R assessments during the day. Twelve months after the EEG and PET assessments, a Glasgow Outcome Scale-Extended (GOS-E) assessment (Wilson *et al.*, 1998) was obtained in collaboration with the patient's referring physician or legal guardian to assess the patient's outcome. Following Stender *et al.* (2014), a GOS-E score threshold of 2 was used to categorize patients as unconscious, i.e. 'outcome-negative' (GOS-E score ≤ 2), or conscious, i.e. 'outcome-positive' (GOS-E score > 2).

PET scans were acquired and interpreted using methodology described in Stender *et al.* (2014) and the Supplementary material. Briefly, complete bilateral hypometabolism of the associative frontoparietal cortex with no voxels with preserved metabolism led to a diagnosis of 'PET-negative', whereas incomplete hypometabolism and partial preservation of activity within these areas yielded a diagnosis of 'PET-positive' (Laureys *et al.*, 2004; Nakayama *et al.*, 2006; Thibaut *et al.*, 2012). PET diagnoses of the first 51 patients listed in Supplementary Table 1 have been included in a previous publication (Stender *et al.*, 2014). EEG data analysis was blinded to the behavioural and PET assessments.

EEG data collection

We collected high density EEG recordings from 256 scalp sensors using a saline electrode net designed by Electric Geodesics (EGI), at a sampling rate of either 250 Hz or 500 Hz (which were down-sampled offline to 250 Hz). Importantly, EEG data were collected during fluorodeoxyglucose (FDG) uptake, for 20–30 min until just before the start of the PET data acquisition, to allow for an accurate comparison of the two modalities. During data collection, we ensured that patients were awake and had their eyes open.

EEG data from nine patients with disorders of consciousness were unusable either due to technical problems, insufficient data, or excessive movement artefacts. Data from 89 patients with disorders of consciousness, 11 emerged from MCS patients, four patients with locked-in syndrome and 26 control subjects were retained for further analysis. After behavioural assessment of the 89 patients with disorders of consciousness with the CRS-R, 23 were diagnosed to be in UWS (Laureys *et al.*, 2010), 17 in MCS–, and 49 in MCS+ (Giacino *et al.*, 2002; Bruno *et al.*, 2011). From each of these patients, we also collected the following demographic details (listed in Supplementary Table 1): age at the time of assessment, days since onset of brain injury that resulted in a disorder of consciousness, aetiology of the injury, specifically traumatic or non-traumatic, and clinical consensus diagnosis (UWS/MCS) as noted by the referring clinical centre.

EEG data analysis

For details of EEG preprocessing and artefact rejection, see Supplementary material. We calculated spectral and cross-spectral decompositions from cleaned high density EEG datasets (Supplementary Fig. 1), using the FieldTrip toolbox (Oostenveld *et al.*, 2011). Power was estimated at bins of 0.1 Hz between 0.5–45 Hz, using a multitaper method with five Slepian tapers. At each channel, magnitude power within three canonical frequency bands, delta (0–4 Hz), theta (4–8 Hz) and alpha (8–13 Hz), were converted to relative percentage contributions to the total power over all three bands. Alongside, the cross-spectrum between the spectral decompositions of every pair of channels was used to calculate the debiased weighted phase lag index (dwPLI) measure (see Supplementary material for further details) introduced by Vinck *et al.* (2011). We used this tried-and-tested measure (Chennu *et al.*, 2014, 2016; Kim *et al.*, 2016) to estimate brain connectivity between pairs of EEG channels in our dataset. Further, we restricted analysis to the delta, alpha and theta bands, as the impact of the considerable electromyographic artefact observed in patients was relatively negligible in these bands. Within each band, dwPLI values at the peak frequency of the oscillatory signal across all channels were used to represent the connectivity between channel pairs. From each subject's dataset, the dwPLI values across all channel pairs were used to construct symmetric 173×173 dwPLI connectivity matrices for the delta, alpha and theta bands.

Brain network analysis

Each dwPLI matrix estimated as above was proportionally thresholded to vary the 'connection density' parameter D , retaining between 90–10% of the largest dwPLI values

(Supplementary Fig. 1). Values below this threshold were set to zero, and non-zero values were set to one, effectively binarizing the thresholded connectivity matrix. This procedure was repeated at each value of connection density D , which ranged between 90% and 10% in steps of 2.5%. At each value of D , the thresholded and binarized matrix was modelled as a network with the electrodes as nodes and non-zero values as edges or connections. These networks were submitted to graph theory algorithms implemented in the Brain Connectivity Toolbox (Rubinov and Sporns, 2010). These algorithms were used to calculate metrics that captured key topological characteristics of the graphs at multiple scales: the microscale clustering coefficient, macro-scale characteristic path length (Watts and Strogatz, 1998), mesoscale modularity (using the Louvain algorithm; Blondel *et al.*, 2008) and participation coefficient (Guimera and Nunes Amaral, 2005). We also calculated the network-level modular span (Chennu *et al.*, 2014), a metric that captures how the topology of the network is embedded in topographical space over the scalp, by combining the community structure estimated by the Louvain algorithm with the normalized distance between channel pairs (see Supplementary material for details of these metrics). While clustering coefficient and participation coefficient were calculated for each node in a network, characteristic path length, modularity and modular span were calculated for the network as a whole. Together, seven metrics were calculated for each frequency band: mean relative power over all channels, median connectivity over all channel pairs, clustering coefficient, characteristic path length, modularity, participation coefficient and modular span. Each of these was calculated in three bands (delta, theta and alpha), making a total of 21 metrics.

The EEG data analysis pipeline detailed above was implemented with MATLAB scripts based on EEGLAB (Delorme and Makeig, 2004). All steps except the identification of excessively noisy channels, epochs, and independent components were completely automated and run in exactly the same way for every EEG dataset, using a fixed set of algorithmic hyperparameters.

Statistical and classification analysis

We used receiver operating characteristic (ROC) analysis to generate area under the curve (AUC) measures to estimate the ability of each of the 21 brain network metrics to discriminate consciousness evidenced by behaviour or PET, and to prognosticate recovery. We calculated the absolute value of the AUC measure between 0.5 and 1, which indicated the extent to which a particular EEG metric discriminated a particular pair of subject groups. A Mann-Whitney test was used to generate a non-parametric P -value quantifying the level of statistical significance associated with an AUC value. Multiple comparisons were accounted for with a false discovery rate correction. The Jonckheere-Terpstra test was used to test for trends in network metrics as a function of the level of behavioural awareness.

Across the 21 metrics estimated from the EEG datasets, the metric that generated the highest AUC for discriminating a pair of subject groups was selected for training a classifier to make predictions about individual patients in the groups. For example, the participation coefficient metric was the best discriminator of UWS versus MCS– diagnosis, while delta band power was the best discriminator of MCS– versus MCS+

diagnosis. These metrics were used to train two-class classifiers to discriminate the respective pairs of patient groups. We used support vector machines (SVMs) with Radial Basis Function kernels to train and cross-validate classifiers (see Supplementary material for details). The input features (columns) for training the classifiers were values of the selected metric at each network node (or the value for the whole network in case of network-level metrics), calculated after thresholding the network at the connection density D that generated the best AUC. The samples (rows) were individual subject networks. The labels corresponding to each sample were either the CRS-R based diagnosis (UWS/MCS–/MCS+), PET-based diagnosis (positive or negative) or GOS-E outcome (positive or negative). For discriminating UWS, MCS– and MCS+ patients from each other, we used Error-Correcting Output Codes (Dietterich and Bakiri, 1995; Allwein *et al.*, 2000) with an exponential loss function to combine two-class classifiers into a three-class classifier. χ^2 tests were used to assess the statistical significance of the match between the labels predicted by the classifiers and the true class labels.

Results

EEG metrics and behavioural awareness

We quantified key properties of each subject's resting brain activity in the delta, theta and alpha bands, organized into increasing levels of analytical depth, namely: mean spectral power over all channels, median spectral connectivity (dwPLI) over all channel pairs, and graph-theoretic metrics including local (clustering coefficient) and global (characteristic path length) efficiency, modularity, intermodular hub strength (participation coefficient) and topographical modular span (see 'Materials and methods' section for details).

Figure 1A plots the resting dwPLI-based alpha band connectivity topographs for each group of patients with disorders of consciousness ordered by increasing level of behavioural responsiveness as quantified by the CRS-R, alongside the emerged from MCS, locked-in syndrome and healthy control groups for comparison. Progressive increase in the strength of EEG connectivity matched the re-emergence of behavioural awareness, with UWS patients showing a prominent lack of structured connectivity. Visually, MCS– and MCS+ patients showed similar levels of connectivity, but the topographical pattern in MCS+ patients showed the presence of a discernible frontoparietal focus for the strongest connections. This pattern was further enhanced in emerged from MCS patients, and was strikingly evident in patients with locked-in syndrome and controls. We have previously demonstrated that such frontoparietal patterns of alpha connectivity are neural markers of behaviourally evidenced consciousness, not only in patients with disorders of consciousness (Chennu *et al.*, 2014), but also during propofol sedation (Chennu *et al.*, 2016). The connectivity patterns in Fig. 1A

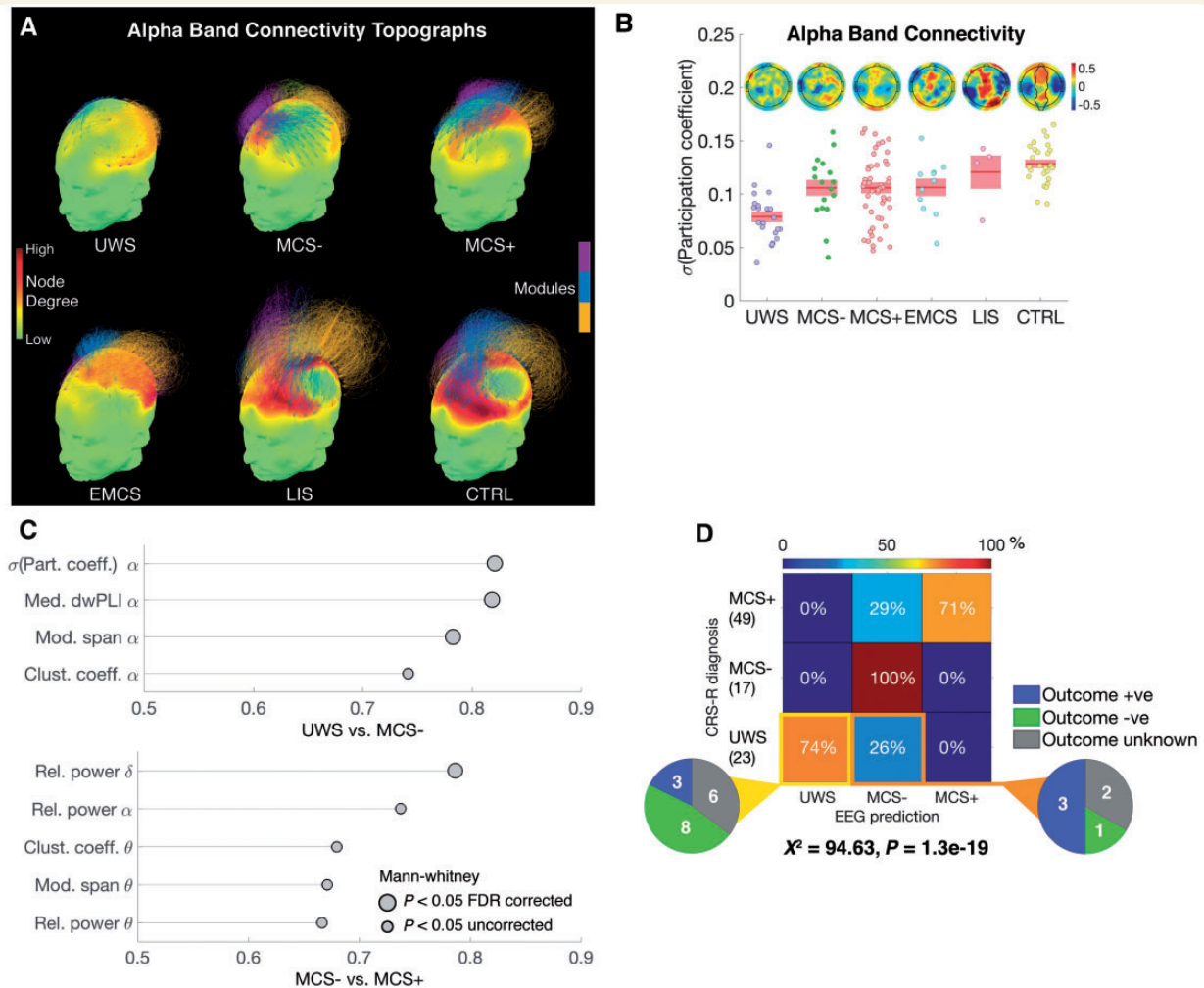


Figure 1 EEG brain networks and levels of consciousness. (A) 3D alpha network topographs for each subject group (see Supplementary Fig. 1 and 'Materials and methods' section for details). Increasing level of consciousness from left to right was correlated with re-emergence of stronger interhemispheric connectivity between frontal and parietal areas. In each topograph, the colour map over the scalp depicts degrees of nodes in the network. Arcs connect pairs of nodes, and their normalised heights indicate the strength of connectivity between them. Topological modules within the network were identified by the Louvain algorithm. For visual clarity, of the strongest 30% of connections, only intramodular connections are plotted. The colour of an arc identifies the module to which it belongs, with groups of arcs in the same colour highlighting connectivity within a module. The standard deviation of participation coefficients over network nodes in each subject's alpha network (B) showed a linear trend with increasing level of consciousness. This metric was averaged over all connection densities considered. In each box in B, the group-wise mean of this metric is indicated by a red line, and standard error of this mean by the red window. Individual patient metrics are shown in the overlaid scatter plot. Above each box, the group-wise mean topoplots of participation coefficient Z-scores highlighted the re-emergence of hub nodes with high participation coefficients in frontal and parietal areas, along with increasing level of consciousness. Rank ordering of the best discriminability achieved between UWS versus MCS– and MCS– versus MCS+, as measured by AUCs (C), highlighted participation coefficient, median connectivity, and modular span metrics, all in the alpha band, as the most effective for discriminating UWS from MCS– patients. Only metrics with significant AUCs are shown (see 'Materials and methods' section for a full list of the 21 metrics estimated from each subject's EEG). For the graph-theoretic metrics, AUC was calculated at each connection density, and the best one obtained is plotted. An SVM trained with cross-validation on patient-wise alpha participation coefficient metrics of UWS, MCS– and MCS+ patients showed significantly above chance

confirmed this finding in a different, much larger and more diverse cohort of patients with disorders of consciousness. However, this analysis of dwPLI-based networks was based on sensor-level EEG data, and hence references to regions allude to areas over the scalp rather than specific regions of underlying brain anatomy.

Figure 1B plots the group-wise distribution of participation coefficients in alpha connectivity networks. For each

group, the figure plots the average topographic distribution of participation coefficient Z-scores. These topoplots depict the re-emergence of hub regions (consisting of nodes with high participation coefficients) in frontal and parietal areas along with increasing levels of awareness. We captured this with the standard deviation of participation coefficients over all nodes, a single scalar metric capturing the diversity of participation coefficients. As shown in Fig. 1B, this

metric demonstrated a statistically significant positive trend with increasing CRS-R diagnosis (Jonckheere-Terpstra trend statistic = 3.26, $P = 0.0006$), and quantified properties that differentiated the networks visualized in Fig. 1A, i.e. the presence of strong connectivity hubs in brain networks. These hubs, supported by pathways of underlying structural connectivity, are thought to create a small-world functional network in the brain (Watts and Strogatz, 1998; Achard *et al.*, 2006). In the context of clinical applications, the topographs and trend in Fig. 1B suggested that assessing the presence of such hubs might be a valuable bedside diagnostic for measuring the potential for consciousness using resting high density EEG data. Additionally, the within-group correlations in the topographical distribution of alpha participation coefficients also increased with CRS-R diagnosis (Jonckheere-Terpstra trend statistic = 2.56, $P = 0.0053$; Supplementary Fig. 2), demonstrating that these brain connectivity hubs were more consistently observed as patients became more behaviourally aware.

Figure 1C plots the results of ROC analyses conducted to estimate the discriminative power of each EEG metric, and depicts only the metrics with statistically significant AUCs in descending rank order (see ‘Materials and methods’ section for the 21 metrics estimated). The top three metrics for discriminating behaviourally evidenced consciousness from the lack thereof, i.e. the UWS versus MCS– categories, were participation coefficient (AUC = 0.83, $P = 0.0006$), median connectivity (AUC = 0.82 Mann-Whitney $P = 0.0007$), and modular span (AUC = 0.78, $P = 0.0026$), all in the alpha band. At the optimal ROC threshold (Youden, 1950) the alpha participation coefficient was 79% accurate in discriminating these two categories ($\chi^2 = 11.52$, $P = 6.9 \times 10^{-4}$). This was comparable with the 81% accuracy ($\chi^2 = 17.15$, $P = 3.4 \times 10^{-5}$) achieved by expert assessment of PET images acquired from the same patients, and also close to the 85% accuracy reported by Stender *et al.* (2014). These connectivity-based measures also outperformed relative alpha power in its ability to discriminate awareness, highlighting that connectivity captured fundamentally distinct information about the neural interactions underlying consciousness. This diagnostic utility of alpha connectivity metrics was preserved within patients with traumatic and non-traumatic aetiologies.

While alpha network metrics were good at distinguishing UWS versus MCS– patients, relative delta band power averaged over all channels was very good at discriminating MCS– from MCS+ patients (AUC = 0.79, $P = 0.0005$). Relative delta power in patients decreased progressively along with increase in their behavioural diagnosis (Jonckheere-Terpstra trend statistic = 3.18, $P = 0.0007$; Supplementary Fig. 4A), potentially reflecting the relative degree of cortical deafferentation (Timofeev *et al.*, 2000; Williams *et al.*, 2013). The presence of this information in the EEG signal enabled us to combine metrics extracted from different frequency bands to accurately place an individual patient along a stratified scale of awareness.

We investigated the generalizability of the above results by training a three-class SVM classifier (see ‘Materials and methods’ section) to predict the diagnosis of individual UWS, MCS– and MCS+ patients. The inputs to the classifier were the subject-wise values of the best performing metrics for discriminating UWS versus MCS– and MCS– versus MCS+, namely alpha participation coefficient and delta band power at each channel. Figure 1D plots the confusion matrix generated by the SVM after stratified cross-validation. A chi-squared test used to statistically estimate the classifier’s performance was highly significant ($\chi^2 = 94.63$, $P = 1.4 \times 10^{-19}$; see Fig. 1D). In particular, as shown in the confusion matrix, it diagnosed UWS, MCS– and MCS+ patients with 74%, 100% and 71% accuracy, all well above the chance level of 33%. Further, the classifier was 100% sensitive to an MCS diagnosis. While a proportion of UWS patients were classified as MCS– (6 of 23), it is possible that these patients had some degree of awareness not evident in their behaviour even with the systematic assessment conducted by the CRS-R (Owen *et al.*, 2006; Monti *et al.*, 2010). A greater proportion (three of six) of such potentially misdiagnosed UWS patients had positive outcomes (mean GOS-E score = 2.75; Fig. 1D) as compared to patients in whom the CRS-R and EEG classifier agreed on a diagnosis of UWS (3 of 17; mean GOS-E score = 2.0). However, the number of patients in these groups was too small to generate sufficient power for statistical analysis of these proportions. Finally, we also found that the classifier generalized very well to previously unseen participation coefficient metrics of emerged from MCS, locked-in syndrome and healthy control subjects, which were not used for training. Specifically, all emerged from MCS patients, locked-in syndrome patients and healthy control subjects were classified as MCS (either MCS– or MCS+).

EEG network centrality correlates with PET metabolism

We investigated whether resting EEG metrics measured at the bedside could predict PET metabolism, to establish the concordance between these very different imaging modalities. We used data from a subset of 98 patients for whom PET scans were available and interpretable. Each patient was first labelled PET-negative or PET-positive using previously established criteria (see ‘Materials and methods’ section, and Stender *et al.*, 2014). Seventeen patients were labelled PET-negative, and the remaining 81 as PET-positive.

Figure 2A plots the average alpha connectivity topographs for PET-negative/positive patients, depicting the striking difference in the strength and pattern of connectivity. Positive metabolism in PET was correlated with strong EEG connectivity between hubs in frontal, parietal and central regions. Indeed, the participation coefficients of these EEG hubs were distinctly higher in PET-positive patients

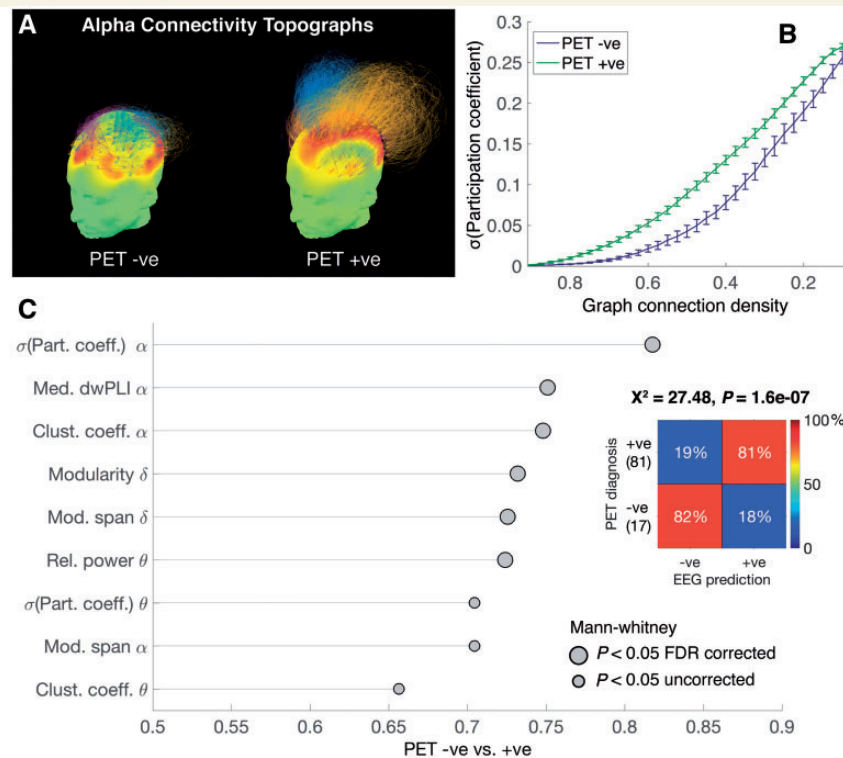


Figure 2 EEG brain networks and PET. Patients were labelled as PET-positive (+ve) based on partial preservation of activity within associative frontoparietal cortex, and PET-negative (–ve) otherwise (Stender *et al.*, 2014). The average EEG alpha network topograph displayed robust connectivity along a frontoparietal axis in PET-positive patients who registered relatively high metabolism (A). Quantitatively, the participation coefficient metric was higher in PET-positive than in PET-negative patients, over a wide range of connection densities (B). This metric was also able to discriminate PET-negative and PET-positive patients better than any other EEG metric, when comparing their AUCs (C). A cross-validated SVM trained on the alpha participation coefficients of patients produced very good performance in predicting their individual PET-based diagnoses, as shown in the confusion matrix in C (inset).

across a wide range of connection density thresholds (Fig. 2B), establishing that the observed difference was not an artefact of the thresholding applied prior to estimation of graph-theoretic metrics.

Using a similar ROC analysis as above, we found that the standard deviation of participation coefficients over the nodes in each patient's alpha network was by far the most discriminative metric, able to distinguish PET-negative/PET-positive patients with an AUC of 0.82 ($P = 4.1 \times 10^{-5}$; Fig. 2C). Further, an SVM classifier trained on this metric performed well ($\chi^2 = 27.48, P = 1.6 \times 10^{-7}$), and was able to identify the PET-based diagnosis of individual patients with high sensitivity (81%) and specificity (82%). Further, as evidence of the classifier's generalizability to previously unseen data, all controls were classified as PET-positive. This suggested that EEG was a reliable bedside predictor of PET activation at an individual patient level. In comparison, the patient's aetiology ($\chi^2 = 3.84, P = 0.05$), days since injury (AUC = 0.56, $P > 0.05$) and age at assessment (AUC = 0.44, $P > 0.05$) did not predict their PET diagnosis.

These results represent strong evidence of the correlation between the presence of highly active and interconnected

hub nodes in functional brain networks measured at the bedside by EEG, and the energetic demands of these hubs, as measured with PET. This is perhaps best exemplified by the comparison of the alpha networks of two demographically similar MCS+ patients in Fig. 3, both of whom were MCS+ after traumatic brain injury. Despite these similarities, however, Patient 79 was PET-negative while Patient 110 was PET-positive, as is evident in their PET scans (Fig. 3A and B). In keeping with this difference in their PET scans, there was a large and obvious difference in their EEG-derived brain networks (Fig. 3C and D). The latter patient had strong, right-lateralized frontoparietal connectivity in their alpha network, which was completely absent in the former.

EEG delta network centrality predicts outcomes

Information about GOS-E outcomes at ~1 year after EEG assessments enabled us to assess the prognostic value of resting EEG network activity in presaging recovery from disorders of consciousness. GOS-E scores of 61 patients

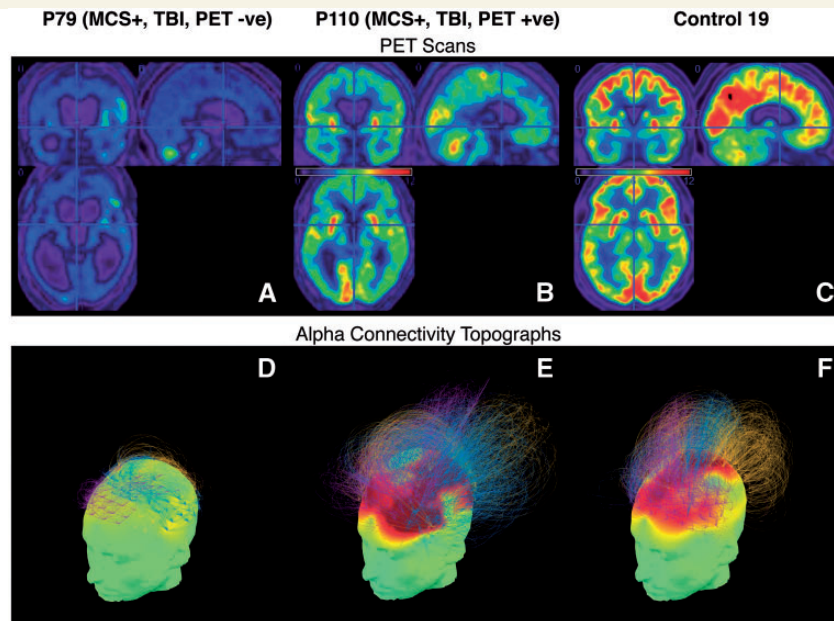


Figure 3 Exemplars of PET-positive and -negative patients. (A and B) PET glucose uptake scans of two subjects (Patients 79 and 110), both of whom were diagnosed as MCS+ after traumatic brain injury. PET-negative (–ve) Patient 79 showed hypometabolism while PET-positive (+ve) Patient 110 had stronger metabolic activity. Their corresponding EEG alpha brain networks (D and E) showed striking differences in the strength of frontoparietal connectivity. PET scan (C) and EEG alpha network (F) of a representative healthy control are shown for comparison.

was available for inclusion into this analysis. Following Stender *et al.* (2014), we dichotomized these GOS-E scores into outcome-positive and outcome-negative. Thirty-nine of the 61 patients had positive outcomes by this definition.

In contrast to the relationship between alpha band connectivity and behavioural/PET diagnosis, we found a clear relationship between delta band connectivity and outcomes. Figure 4A shows delta band network connectivity topographs averaged over patients with positive and negative outcomes. Strong connections across large parts of central and parietal areas were prominent in patients who eventually had negative outcomes as per the GOS-E. In contrast, patients who had positive outcomes had diminished delta connectivity (Fig. 4A, right).

We separated patients with non-traumatic ($n = 53$) and traumatic aetiologies ($n = 51$) to explore this relationship between delta connectivity and outcomes quantitatively. Patients with positive outcomes after non-traumatic brain injury had higher mesoscale modularity, highlighting the maladaptive nature of delta connectivity and the loss of strong synchronous oscillations in the delta band as a positive predictor of recovery (Supplementary Fig. 4B). Patients with positive outcomes after traumatic injury had higher microscale clustering coefficients in their delta networks, suggesting local topological connectivity in the delta band was a positive predictor in this group (Fig. 4B). These two delta band metrics significantly predicted outcomes (Fig. 4C), with an AUC of 0.77 ($P = 0.015$) and 0.78

($P = 0.019$) in non-traumatic and traumatic aetiologies, respectively. We also found that standard deviation of participation coefficients in delta band networks was the best discriminator of aetiology itself (AUC = 0.67, $P = 0.003$) (Supplementary Fig. 5).

Demographic factors like the patient's age also predicted outcome (AUC = 0.72, $P = 0.030$), as did aetiology itself ($\chi^2 = 4.35$, $P = 0.040$). The ability of the CRS-R total score to predict outcomes was similar (AUC = 0.66, $P = 0.038$), as was the case with the CRS-R based UWS/MCS diagnosis (accuracy = 69%, $\chi^2 = 4.94$, $P = 0.026$). This finding highlights EEG network metrics as valuable predictors of recovery that can complement demographic and behavioural information.

We constructed SVM classifiers trained with cross-validation on the above two metrics, namely delta modularity and clustering coefficients. They were able to significantly predict future GOS-E dichotomized outcomes in individual patients (accuracy = 82%, $\chi^2 = 21.89$, $P = 2.9 \times 10^{-6}$) better than the CRS-R diagnosis, and closely matched the predictive strength of PET-based diagnosis (accuracy = 81%, $\chi^2 = 19.05$, $P = 1.3 \times 10^{-5}$). Figure 4C (inset) depicts the confusion matrix generated, which produced 92% sensitivity and 64% specificity in discriminating positive and negative outcomes. Further, we verified that the classifier was able to predict outcomes within the subgroups of UWS and MCS patients with 80% and 87% accuracy, respectively, confirming its prognostic utility within these CRS-R diagnoses.

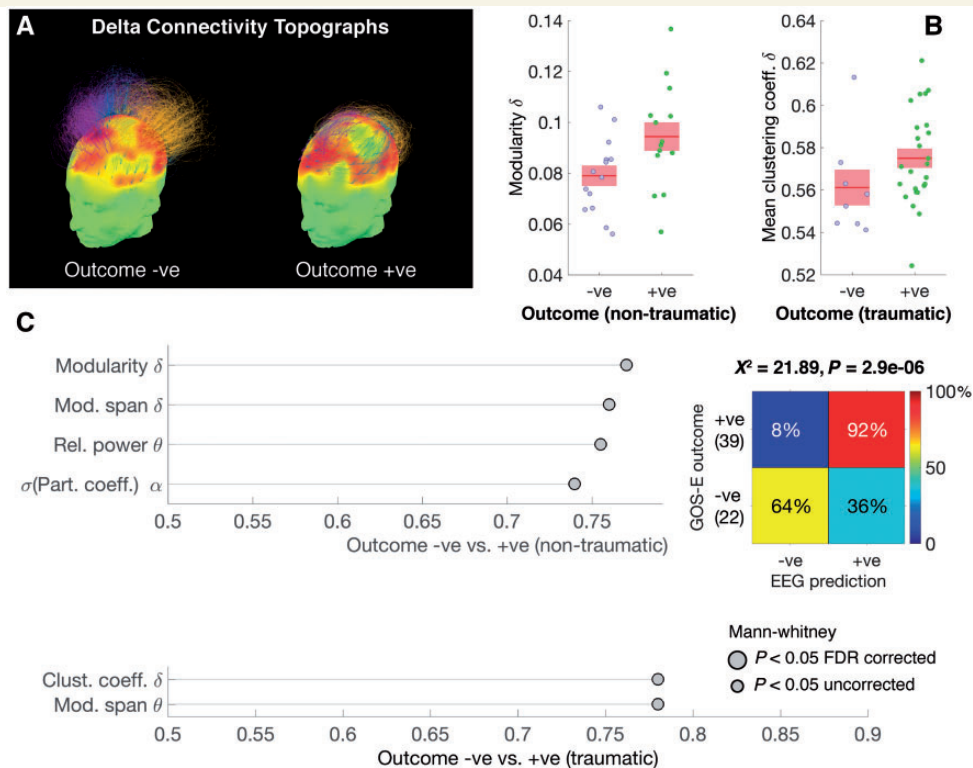


Figure 4 EEG networks and outcomes. Patients were labelled as outcome-positive (+ve) if their 1-year GOS-E score was > 2 , and outcome-negative (–ve) otherwise (Stender *et al.*, 2014). Delta networks were stronger in patients with negative outcomes (A), indicating synchronized delta band oscillations across many EEG electrodes. The modularity (non-traumatic injury) and clustering coefficients (traumatic injury) of delta networks were higher in patients with positive outcomes. (B). These metrics were best able to discriminate positive and negative outcomes in both aetiologies, as measured by AUC (C). When used to train a cross-validated SVM, they contributed to significant performance in predicting individual patient outcomes (C, inset).

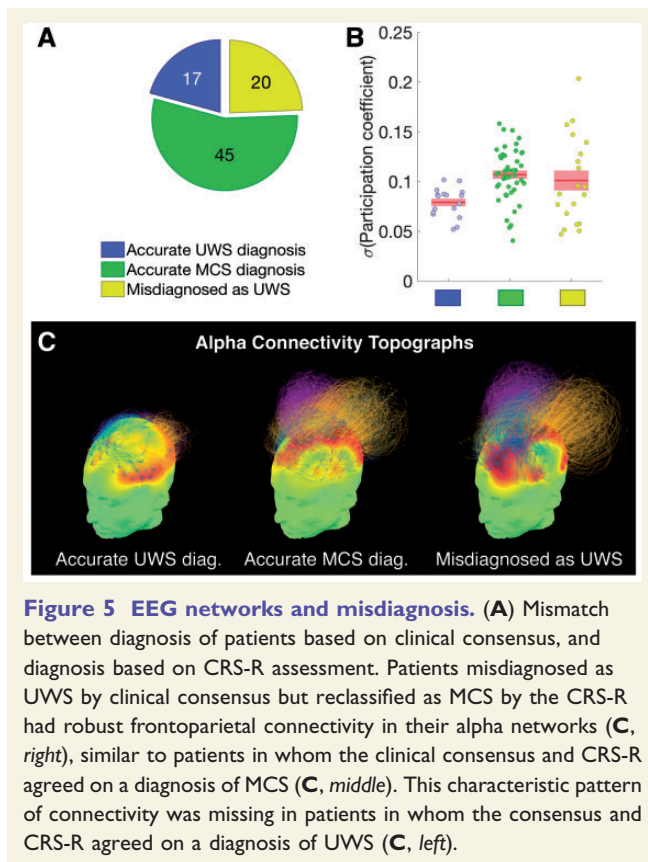
EEG network centrality can improve clinical diagnostics

Eighty-two patients had a diagnosis available at referral, as ascertained by clinical consensus. This consensus diagnosis was either UWS/vegetative or MCS. We compared these to the CRS-R diagnoses during the week of hospitalization to identify three groups of patients: 17 whose consensus diagnosis of UWS agreed with their CRS-R based UWS diagnosis, 45 whose consensus diagnosis of MCS agreed with their CRS-R based MCS diagnosis, and 20 who had been misdiagnosed as UWS, relative to their MCS diagnosis when reassessed with the CRS-R (Fig. 5A). Hence 20 of 37 patients who were UWS as per their consensus diagnosis were reclassified as MCS after reassessment with the CRS-R.

We examined whether EEG assessments of brain networks, if available at the bedside, could help inform more accurate diagnoses. Figure 5C plots the alpha network connectivity topographs averaged over patients in the three groups above. It was evident that patients who had been misdiagnosed as UWS by clinical consensus (Fig. 5C, right) had robust frontoparietal brain networks

similar to patients who had been correctly diagnosed as MCS (Fig. 5C, middle), and dissimilar to patients correctly diagnosed as UWS (Fig. 5C, left). To quantify this visual pattern, Fig. 5B plots the standard deviation over participation coefficients of these networks. In keeping with the intuition from the visualizations in Fig. 5C, the patients misdiagnosed as UWS had significantly higher values of this metric than patients who were indeed in UWS as per the CRS-R ($U = 87, P = 0.01$). In fact, we did not find significant differences between patients correctly diagnosed as MCS and those misdiagnosed as UWS, in any of the 21 metrics we estimated.

Finally, we evaluated whether the classifier we previously constructed to distinguish between the UWS, MCS– and MCS+ categories was able to detect the misdiagnosis of consciousness. We found that all 20 patients misdiagnosed as UWS were classified as MCS– or MCS+ by the EEG-based classifier. That is, the presence of hub nodes in the alpha network, as measured by participation coefficients, was able to diagnose the presence of consciousness in patients who had been misdiagnosed as UWS based on clinical consensus.



Discussion

Our findings have described how EEG-derived networks of electrical activity in patients are associated with behavioural consciousness, the metabolic demand of the brain, and clinical outcomes. Further, we have demonstrated that this association is robust enough to build reliable predictors of behavioural diagnosis, PET diagnosis and outcomes in individual patients. In doing so, we have set out the evidence base to evaluate the key questions articulated in the Introduction, which are important for demonstrating the clinical utility of EEG-based assessments in disorders of consciousness.

First, our results have reiterated the positive link between sensor-level connectivity in the alpha band and conscious states indexed by behaviour. We have shown that the progressive re-emergence of connectivity hubs in EEG brain networks, as measured by participation coefficients, tracks the consistency with which consciousness can be measured with the CRS-R, with accuracy comparable to PET-based assessment by an expert. Indeed, the notion that connectivity hubs in specific frontal and parietal loci are important for the recovery of consciousness after brain injury is consistent with evidence from both PET (Stender *et al.*, 2014, 2015, 2016) and functional MRI (Vanhaudenhuyse *et al.*, 2010b; Achard *et al.*, 2012). Further, as patients recover

beyond MCS, it appears that both positive and negative correlations of activity within and between networks also reappear (Thibaut *et al.*, 2012; Di Perri *et al.*, 2016). This relationship between the complexity of activity in brain networks and the state of consciousness has been demonstrated across mechanistically diverse natural, pharmacological and pathological modulations of consciousness using transcranial magnetic stimulation (TMS, Casali *et al.*, 2013; Casarotto *et al.*, 2016) as well as resting state EEG (Schartner *et al.*, 2015). Further, recent literature has highlighted high frequency (20–50 Hz) activity in the parietal cortex (a ‘posterior hot zone’) as a neural correlate of conscious contents (Koch *et al.*, 2016; Siclari *et al.*, 2017). We complement this finding by highlighting frontoparietal connectivity in the alpha band as a potential correlate of the level of consciousness.

Our finding is also consistent with previous literature that analysed EEG data with complementary methods based on clinical expertise (Forgacs *et al.*, 2014) and information theory (King *et al.*, 2013). This engenders confidence in the reliability of EEG as a valuable tool, as it suggests that different analytical methods could be used to deliver similarly capable diagnostic capabilities. Further, the strength of the relationship between the best brain network metrics we use here and the CRS-R based diagnosis is comparable to that reported in previous literature that has employed EEG-based analysis (King *et al.*, 2013; Sitt *et al.*, 2014). PET (Stender *et al.*, 2016) and TMS-EEG (Casarotto *et al.*, 2016) have been shown to perform better, but both require much more complex technology that is either impossible or difficult to deploy at the patient’s bedside. Hence bedside EEG assessments of brain connectivity, potentially estimated with fewer sensors than the high density configuration employed here (Engemann *et al.*, 2015), could valuably complement other neuroimaging technologies. Indeed, we replicated the finding by Engemann *et al.* (2015) that the positive trend in median dwPLI connectivity alongside increasing behavioural diagnosis is relatively robust against a progressive reduction in the number of electrodes included (Supplementary Fig. 3). Going further, we evaluated the usefulness of a subset of frontal and parietal electrodes, delineated by the regions with high participation coefficients seen in conscious healthy controls (Fig. 1B, healthy controls topoplots). Connectivity within this spatially circumscribed subset of electrodes demonstrated a stronger trend with the level of consciousness as compared to an evenly distributed configuration with a similar number of electrodes. This suggested that customized placement over connectivity hubs could reduce the number of electrodes needed, while also preserving discriminative power and clinical utility of the signals measured.

Second, we have shown that there is also a strong association between the presence of EEG-based brain connectivity hubs and glucose metabolism itself. PET is an established tool in clinical imaging, and recent advances in clinical neuroimaging in disorders of consciousness have highlighted the potential for brain metabolism

measured by PET imaging to diagnose the level of consciousness (Stender *et al.*, 2014, 2016). This previous research has shown that normal metabolic activity in key brain areas including lateral and medial frontoparietal networks are strong predictors of the level of behavioural consciousness indexed by the CRS-R, and even the recovery thereof. Further, this evidence has been linked with the notion that these brain areas are considered to be key connectivity hubs supporting internal (self) and external (stimulus) awareness (Vanhaudenhuyse *et al.*, 2010a). Building on this work, we studied the relationship between EEG and PET in disorders of consciousness, ensuring that the two modalities could be reliably correlated by performing EEG assessments during the period of FDG uptake. The concordance we have demonstrated between EEG and PET builds confidence in the basis of the EEG assessments, which could eventually be deployed at the patient's bedside. Though EEG cannot provide the same kind of information as that can be inferred from PET, our findings provide evidence for a consilience-based approach to diagnosis in the absence of a gold-standard test for consciousness (Peterson, 2016). Convergent with this approach, Bodart *et al.* (2017) recently demonstrated a strong correspondence between PET and the complexity of TMS responses measured with EEG. Their findings strengthen the conceptual basis of the link between EEG-derived network metrics and PET metabolism demonstrated here. Here, we have exploited this evidence to train classifiers that predict the PET diagnosis of individual patients based on the presence of connectivity hubs measured with resting EEG.

Third, in contrast to the positive association between increasing alpha network connectivity and behavioural diagnosis, we have shown that there is a significant link between maladaptive delta band connectivity in EEG brain networks and outcomes. This link was modulated by the aetiology of brain injury and the potential extent of partial deafferentation of cortical and subcortical neurons (Williams *et al.*, 2013) known to produce oscillations within the delta band (Timofeev *et al.*, 2000). This knowledge could be valuable for ensuring the timeliness of pharmacological interventions that can accelerate positive outcomes (Giacino *et al.*, 2012). We propose that repeated and regular bedside EEG assessments would cover a greater range of arousal fluctuations, would improve our ability to accurately track and predict the recovery of consciousness in individual patients. Indeed, Casarotto *et al.* (2016) have shown that taking the maximum value of the complexity of brain activity measured over multiple TMS-EEG assessments can considerably improve the reliability of the estimation. Hence, developing a framework and analytical pipeline for repeatable bedside assessments could enable robust estimation of EEG-based metrics for quantifying brain networks in disorders of consciousness.

With regard to repeatable assessments, it is worth pointing out that despite the complexity of the network analysis and classification algorithms we have presented here, these steps are completely automated from an application

perspective. We highlight relevant work by Sitt *et al.* (2014), who conducted a comprehensive analysis of a large number of measures from high density EEG to test their ability to discriminate UWS from MCS. These measures included event-related potentials, spectral power, connectivity, entropy, complexity and mutual information, amongst others. They showed that different measures extracted from EEG signals could be beneficially combined to build automated tools for discriminating consciousness in patients. Our results concur with and complement their work, demonstrating that brain networks estimated at rest can also predict the stratified level of consciousness in patients, their brain metabolism, and their clinical outcomes. However, a current limitation of the EEG-based assessments proposed here stems from expert intervention required for artefact removal, specifically for inspecting and identifying noisy data and independent components. There have been many recent methodological advances in automating this step (Nolan *et al.*, 2010; Mognon *et al.*, 2011; Jas *et al.*, 2016), and future work towards validating these methods with patient datasets could help develop the analytical pipeline for clinical applications.

Finally, juxtaposing patients misdiagnosed as UWS by clinical consensus against those correctly diagnosed as MCS, we have highlighted the value of EEG in complementing behavioural assessment with the CRS-R. The CRS-R has been shown to considerably improve on standard clinical examination by performing an assessment of behaviour, and thereby reduce the risk of misdiagnosis (Schnakers *et al.*, 2009). However, a well-trained expert is required to apply the CRS-R consistently and reliably (Løvstad *et al.*, 2010), and EEG-based assessments could complement such expert knowledge. In doing so, they could provide treating clinicians with multiple sources of convergent evidence for better diagnosis and prognosis, and for evaluating the effectiveness of specific interventions.

Acknowledgements

We would like to thank the patients, their families, carers and treating clinicians for their participation in this study.

Funding

The authors received funding from the UK Engineering and Physical Sciences Research Council (EP/P033199/1), Evelyn Trust (Cambridge, UK), the UK National Institute for Health Research (NIHR) as part of the Acute Brain Injury and Repair Theme of the Cambridge Biomedical Research Centre, the NIHR Brain Injury Healthcare Technology Cooperative, the NIHR Senior Investigator award, the James S. McDonnell Foundation, the Belgian National Fund for Scientific Research (FNRS), the European Commission, the Human Brain Project (EU-H2020-fetflagship-hbp-sga1-ga720270), the Luminous

project (EU-H2020-fetopen-ga686764), the French Speaking Community Concerted Research Action, the Belgian American Educational Foundation, the Wallonie-Bruxelles Federation, the European Space Agency, the University and University Hospital of Liège (Belgium).

Supplementary material

Supplementary material is available at *Brain* online.

References

- Achard S, Delon-Martin C, Vértes PE, Renard F, Schenck M, Schneider F, et al. Hubs of brain functional networks are radically reorganized in comatose patients. *Proc Natl Acad Sci USA* 2012; 109: 20608–13.
- Achard S, Salvador R, Whitcher B, Suckling J, Bullmore E. A resilient, low-frequency, small-world human brain functional network with highly connected association cortical hubs. *J Neurosci* 2006; 26: 63–72.
- Allwein EL, Schapire RE, Singer Y. Reducing multiclass to binary: a unifying approach for margin classifiers. *J Mach Learn Res* 2000; 1: 113–41.
- Bagnato S, Boccagni C, Prestandrea C, Fingelkurts AA, Fingelkurts AA, Galardi G. Changes in standard electroencephalograms parallel consciousness improvements in patients with unresponsive wakefulness syndrome. *Arch Phys Med Rehabil* 2016; 98: 665–72.
- Blondel VD, Guillaume J-L, Lambiotte R, Lefebvre E. Fast unfolding of communities in large networks. *J Stat Mech Theory Exp* 2008; 2008: P10008.
- Bodart O, Gosseries O, Wannez S, Thibaut A, Annen J, Boly M, et al. Measures of metabolism and complexity in the brain of patients with disorders of consciousness. *Neuroimage Clin* 2017; 14: 354–62.
- Bruno MA, Vanhaudenhuyse A, Thibaut A, Moonen G, Laureys S. From unresponsive wakefulness to minimally conscious PLUS and functional locked-in syndromes: recent advances in our understanding of disorders of consciousness. *J Neurol* 2011; 258: 1373–84.
- Casali AG, Gosseries O, Rosanova M, Boly M, Sarasso S, Casali KR, et al. A theoretically based index of consciousness independent of sensory processing and behavior. *Sci Transl Med* 2013; 5: 198ra105.
- Casarotto S, Comanducci A, Rosanova M, Sarasso S, Fecchio M, Napolitani M, et al. Stratification of unresponsive patients by an independently validated index of brain complexity. *Ann Neurol* 2016; 80: 718–29.
- Chennu S, Finoia P, Kamau E, Allanson J, Williams GB, Monti MM, et al. Spectral signatures of reorganised brain networks in disorders of consciousness. *PLoS Comput Biol* 2014; 10: e1003887.
- Chennu S, O'Connor S, Adapa R, Menon DK, Bekinschtein TA. Brain connectivity dissociates responsiveness from drug exposure during propofol-induced transitions of consciousness. *PLoS Comput Biol* 2016; 12: e1004669.
- Childs NL, Mercer WN, Childs HW. Accuracy of diagnosis of persistent vegetative state. *Neurology* 1993; 43: 1465–7.
- Delorme A, Makeig S. EEGLAB: an open source toolbox for analysis of single-trial EEG dynamics including independent component analysis. *J Neurosci Methods* 2004; 134: 9–21.
- Demertzi A, Antonopoulos G, Heine L, Voss HU, Crone JS, de Los Angeles C, et al. Intrinsic functional connectivity differentiates minimally conscious from unresponsive patients. *Brain* 2015; 138: 2619–31.
- Di Perri C, Bahri MA, Amico E, Thibaut A, Heine L, Antonopoulos G, et al. Neural correlates of consciousness in patients who have emerged from a minimally conscious state: a cross-sectional multimodal imaging study. *Lancet Neurol* 2016; 15: 830–42.
- Dietterich TG, Bakiri G. Solving multiclass learning problems via error-correcting output codes. *J Artif Int Res* 1995; 2: 263–86.
- Engemann D, Raimondo F, King J-R, Jas M, Gramfort A, Dehaene S, et al. Automated measurement and prediction of consciousness in vegetative and minimally conscious patients. In: *ICML workshop on statistics, machine learning and neuroscience 2015*. Lille, France; 2015.
- Estraneo A, Loreto V, Guarino I, Boemia V, Paone G, Moretta P, et al. Standard EEG in diagnostic process of prolonged disorders of consciousness. *Clin Neurophysiol* 2016; 127: 2379–85.
- Forgacs PB, Conte MM, Fridman EA, Voss HU, Victor JD, Schiff ND. Preservation of electroencephalographic organization in patients with impaired consciousness and imaging-based evidence of command-following. *Ann Neurol* 2014; 76: 869–79.
- Giacino JT, Ashwal S, Childs N, Cranford R, Jennett B, Katz DI, et al. The minimally conscious state: definition and diagnostic criteria. *Neurology* 2002; 58: 349–53.
- Giacino JT, Whyte J, Bagiella E, Kalmar K, Childs N, Khademi A, et al. Placebo-controlled trial of amantadine for severe traumatic brain injury. *N Engl J Med* 2012; 366: 819–26.
- Guimera R, Nunes Amaral LA. Functional cartography of complex metabolic networks. *Nature* 2005; 433: 895–900.
- Jas M, Engemann DA, Bekhti Y, Raimondo F, Gramfort A. Autoreject: automated artifact rejection for MEG and EEG data. *ArXiv* 2016. eprint arXiv:1612.08194.
- Kalmar K, Giacino JT. The JFK coma recovery scale - revised. *Neuropsychol Rehabil* 2005; 15: 454–60.
- Kim M, Mashour GA, Moraes SB, Vanini G, Tarnal V, Janke E, et al. Functional and topological conditions for explosive synchronization develop in human brain networks with the onset of anesthetic-induced unconsciousness. *Front Comput Neurosci* 2016; 10: 1.
- King JR, Sitt JD, Faugeras F, Rohaut B, El Karoui I, Cohen L, et al. Information sharing in the brain indexes consciousness in noncommunicative patients. *Curr Biol* 2013; 23: 1914–9.
- Koch C, Massimini M, Boly M, Tononi G. Neural correlates of consciousness: progress and problems. *Nat Rev Neurosci* 2016; 17: 307–21.
- Laureys S, Celesia GG, Cohadon F, Lavrijsen J, León-Carrión J, Sannita WG, et al. Unresponsive wakefulness syndrome: a new name for the vegetative state or apallic syndrome. *BMC Med* 2010; 8: 68.
- Laureys S, Owen AM, Schiff ND. Brain function in coma, vegetative state, and related disorders. *Lancet Neurol* 2004; 3: 537–46.
- Lechinger J, Bothe K, Pichler G, Michitsch G, Donis J, Klimesch W, et al. CRS-R score in disorders of consciousness is strongly related to spectral EEG at rest. *J Neurol* 2013; 260: 2348–56.
- Lehembre R, Marie-Aurèle B, Vanhaudenhuyse A, Chatelle C, Cologan V, Leclercq Y, et al. Resting-state EEG study of comatose patients: a connectivity and frequency analysis to find differences between vegetative and minimally conscious states. *Funct Neurol* 2012; 27: 41–7.
- Løvstad M, Frøslie KF, Giacino JT, Skandsen T, Anke A, Schanke A-K. Reliability and diagnostic characteristics of the JFK coma recovery scale-revised: exploring the influence of Rater's level of experience. *J Head Trauma Rehabil* 2010; 25: 349–56.
- Mognon A, Jovicich J, Bruzzone L, Buiatti M. ADJUST: an automatic EEG artifact detector based on the joint use of spatial and temporal features. *Psychophysiology* 2011; 48: 229–40.
- Monti MM, Vanhaudenhuyse A, Coleman MR, Boly M, Pickard JD, Tshibanda L, et al. Willful modulation of brain activity in disorders of consciousness. *N Engl J Med* 2010; 362: 579–89.
- Nakayama N, Okumura A, Shinoda J, Nakashima T, Iwama T. Relationship between regional cerebral metabolism and consciousness disturbance in traumatic diffuse brain injury without large focal lesions: an FDG-PET study with statistical parametric mapping analysis. *J Neurol Neurosurg Psychiatry* 2006; 77: 856–62.

- Nolan H, Whelan R, Reilly RB. FASTER: fully automated statistical thresholding for EEG artifact rejection. *J Neurosci Methods* 2010; 192: 152–62.
- Oostenveld R, Fries P, Maris E, Schoffelen J-M. FieldTrip: open source software for advanced analysis of MEG, EEG, and invasive electrophysiological data. *Comput Intell Neurosci* 2011; 2011: 156869.
- Owen AM, Coleman MR, Boly M, Davis MH, Laureys S, Pickard JD. Detecting awareness in the vegetative state. *Science* 2006; 313: 1402.
- Peterson A. Consilience, clinical validation, and global disorders of consciousness: Table 1. *Neurosci Conscious* 2016; 2016: niw011.
- Peterson A, Cruse D, Naci L, Weijer C, Owen AM. Risk, diagnostic error, and the clinical science of consciousness. *Neuroimage Clin* 2015; 7: 588–97.
- Piarulli A, Bergamasco M, Thibaut A, Cologan V, Gosseries O, Laureys S. EEG ultradian rhythmicity differences in disorders of consciousness during wakefulness. *J Neurol* 2016; 263: 1746–60.
- Rubinov M, Sporns O. Complex network measures of brain connectivity: uses and interpretations. *Neuroimage* 2010; 52: 1059–69.
- Schartner M, Seth A, Noirhomme Q, Boly M, Bruno MA, Laureys S, et al. Complexity of multi-dimensional spontaneous EEG decreases during propofol induced general anaesthesia. *PLoS One* 2015; 10: e0133532.
- Schnakers C, Vanhaudenhuyse A, Giacino J, Ventura M, Boly M, Majerus S, et al. Diagnostic accuracy of the vegetative and minimally conscious state: clinical consensus versus standardized neurobehavioral assessment. *BMC Neurol* 2009; 9: 35.
- Siclari F, Baird B, Perogamvros L, Bernardi G, LaRocque JJ, Riedner B, et al. The neural correlates of dreaming. *Nat Neurosci* 2017; 20: 872–8.
- Sitt JD, King JR, El Karoui I, Rohaut B, Faugeras F, Gramfort A, et al. Large scale screening of neural signatures of consciousness in patients in a vegetative or minimally conscious state. *Brain* 2014; 137: 2258–70.
- Stender J, Gosseries O, Bruno M-A, Charland-Verville V, Vanhaudenhuyse A, Demertzi A, et al. Diagnostic precision of PET imaging and functional MRI in disorders of consciousness: a clinical validation study. *Lancet* 2014; 384: 514–22.
- Stender J, Kupers R, Rodell A, Thibaut A, Chatelle C, Bruno MA, et al. Quantitative rates of brain glucose metabolism distinguish minimally conscious from vegetative state patients. *J Cereb Blood Flow Metab* 2015; 35: 58–65.
- Stender J, Mortensen Kristian N, Thibaut A, Darkner S, Laureys S, Gjedde A, et al. The minimal energetic requirement of sustained awareness after brain injury. *Curr Biol* 2016; 26: 1494–9.
- Thibaut A, Bruno MA, Chatelle C, Gosseries O, Vanhaudenhuyse A, Demertzi A, et al. Metabolic activity in external and internal awareness networks in severely brain-damaged patients. *J Rehabil Med* 2012; 44: 487–94.
- Timofeev I, Grenier F, Bazhenov M, Sejnowski TJ, Steriade M. Origin of slow cortical oscillations in deafferented cortical slabs. *Cereb Cortex* 2000; 10: 1185–99.
- Vanhaudenhuyse A, Demertzi A, Schabus M, Noirhomme Q, Bredart S, Boly M, et al. Two distinct neuronal networks mediate the awareness of environment and of self. *J Cogn Neurosci* 2010a; 23: 570–8.
- Vanhaudenhuyse A, Noirhomme Q, Tshibanda LJ-F, Bruno M-A, Boveroux P, Schnakers C, et al. Default network connectivity reflects the level of consciousness in non-communicative brain-damaged patients. *Brain* 2010b; 133: 161–71.
- Vinck M, Oostenveld R, van Wingerden M, Battaglia F, Pennartz CM. An improved index of phase-synchronization for electrophysiological data in the presence of volume-conduction, noise and sample-size bias. *Neuroimage* 2011; 55: 1548–65.
- Watts DJ, Strogatz SH. Collective dynamics of ‘small-world’ networks. *Nature* 1998; 393: 440–2.
- Williams ST, Conte MM, Goldfine AM, Noirhomme Q, Gosseries O, Thonnard M, et al. Common resting brain dynamics indicate a possible mechanism underlying zolpidem response in severe brain injury. *eLife* 2013; 2: e01157.
- Wilson JTL, Pettigrew LEL, Teasdale GM. Structured interviews for the glasgow outcome scale and the extended glasgow outcome scale: guidelines for their use. *J Neurotrauma* 1998; 15: 573–85.
- Youden WJ. Index for rating diagnostic tests. *Cancer* 1950; 3: 32–5.